Fluorescence Micrograph Segmentation by Gestalt-Based Feature Binding

Tim W. Nattkemper,[1] Heiko Wersing,[1]
Helge Ritter,[1] Walter Schubert[2,3]

[1]Neuroinformatics Group, University of Bielefeld, Germany,
email: {tnattkem,hwersing,helge}@techfak.uni-bielefeld.de
[2]Neuroimmunology and Molecular Pattern Recognition Group, University of Magdeburg
[3]MELTEC Ltd., University of Magdeburg, email:schubert@pc.mdlink.de

Abstract

We present the application of a recurrent neural network feature binding model to the segmentation of fluorescence micrographs, images showing fluorescent cells in tonsil tissue. Image primitives, referred to as *features*, consisting of position and local gradient information, build the input to the model. The competitive layer model is used to provide a binding of features to convex groups, corresponding to fluorescent cell bodies. Although the images contain noise, and the cells' shapes show considerable variation, the fluorescent cell contours are extracted with sufficient accuracy, according to the biomedical expert. The method achieves at the same time grouping and figure-ground segmentation, and does not require to manually fix the number of groups.

1 Introduction

In the last years the automation of sample preparation and microscopy imaging in biological experiments led to a an enormous increase of digitized image data. In many cases one deals with noisy intensity images, showing objects of same cellular type, but of varying contour. In this work we face the problem of evaluating micrographs,showing fluorescent cell bodies in front of an heterogenous background (tissue). The micrographs are grey value images, recorded by a CCD camera-equipped microscope. The images presented in this paper were recorded by the biomedical research group at the University of Magdeburg and the presented works were done in a close collaboration with the experts of this group. As a basis for later data analysis each image has to be segmented into separately labeled regions, occupied by fluorescent cells, and the background. The fluorescent cell contours have to be approximated to analyze fluorescence intensity distribution across the cell body. Additionally the contour formation of a cell can give information about its migration target. Evaluation of a large number of these micrographs by human employees is practically impossible, because visual inspection of noisy intensity images is tiresome. The observer's concentration decreases after a few minutes so evaluation of the image data by employees is often not only time consuming but leads to non-reproducible results. The automation of the evaluation of the noisy microscope images showing cells of varying contour is an interesting field for the application of artifical neural nets.

Image segmentation into salient groups is a fundamental task in machine vision. The main reason for this is that grouping seems to be a necessary step for guiding recognition processes in general. After the image is segmented to groups those can be used to guide the image interpretation [Lowe, 1985]. The saliency of a group is often measured due to the gestalt principles of perception [Kohler, 1959] like symmetry, good continuation or co-circularity and feature binding has been considered as an elegant approach to Gestalt grouping. In this paper we present an approach for binding those features to salient groups which obey co-circularity and convexity. Image segmentation is interpreted as the process of *binding* image primitives, referred to as *features*, to salient groups. The features consist of image coordinates and orientation of the intensity gradients. The binding is provided by an energy-based recurrent network of competitive layer model type (CLM) [Ritter, 1990],[Wersing et al., 1997]. The result of this *grouping* is a segmentation into background and separated groups of image features, representing image regions, occupied by fluorescent cells. In the CLM, binding is achieved by a spatial process in a set of layers with topographically organized competitive and cooperative interactions of features. The stable attractors of the CLM dynamics can be interpreted as feasible solutions to the labeling or binding problem. The central advantages of the CLM approach are (i) good controllability of the desired groupings due to the presence of an energy function , (ii) the possibility of combined figure-ground segmentation and grouping, (iii) robust representation of multiple groups, where the number is not fixed beforehand, and (iv) a computer implementation with a fast converging asynchronous iteration routine.

Other recent models of feature binding in contour processing have only considered figure ground segmentation ([Yen and Finkel, 1998], [Li, 1999]). Segmentation algorithms in related computer vision applications are for example based on (i) flooding schemes in gradient mountains [Meyer and Beucher, 1990], (ii) wave propagation [Hanahara and Hiyane, 1990], (iii) boundary tracing [Galbraith et al., 1991] or (iv) backtracking search through combinations of line segments by calculating a saliency measure [Jacobs, 1996]. In our present study the considered objects are lymphocytes during a migration in tissue, so their shapes show considerable variation and their shape is called *mainly convex*. This makes it very difficult to define one common contour model, which fits for all cells in the image. Furthermore, since the images are generated by immunofluorescence labeling the resulting images are noisy because of heterogenous signals reflecting different concentrations of cell surface proteins. Because of this heterogenous fluorescence behavior an intensity binarization, necessary for (iii) and (iv), would be a non-trivial task. Thus, the above approaches seem unsuitable for our scenario.

2 The CLM architecture

The CLM consists of a set of L identical layers of feature-selective neurons which are replicas of one input layer (see Fig. 1(a)). The neurons in the input layer are numbered by r and the layers by α. Driven by an external image input, each input neuron responds with a value h_r which indicates activity ($h_r > 0$) in the presence of the corresponding feature r or silence ($h_r \leq 0$). For each of the input neurons at position r there is one neuron per replica layer α whose activity is $x_{r\alpha} \geq 0$ and represents the certainty of assigning feature r to layer α. A feature r is described by an associated parameter vector ν_r. In image processing applications this can be x, y-position, grey value or intensity gradient. We denote the subset of L neurons $x_{r\alpha}$, responding to feature ν_r as the *column* col_r. The activities are subject to the following constrained gradient dynamics:

$$\dot{x}_{r\alpha} = -\frac{\partial E}{\partial x_{r\alpha}} = J(h_r - \sum_\beta x_{r\beta}) + \sum_{r'} \mathsf{f}^\alpha_{rr'} x_{r'\alpha} - T\ x_{r\alpha} \quad , \tag{1}$$

subject to $x_{r\alpha} \geq 0$, where the energy is given by

$$E = \frac{J}{2} \sum_r \Big(\sum_\alpha x_{r\alpha} - h_r \Big)^2 - \frac{1}{2} \sum_\alpha \sum_{rr'} \mathsf{f}^\alpha_{rr'} x_{r\alpha} x_{r'\alpha} + \frac{1}{2} T \sum_{r\alpha} x^2_{r\alpha} \quad . \tag{2}$$

J and T are positive constants and $\mathsf{f}^\alpha_{rr'} = \mathsf{f}^\alpha_{r'r}$ are the components of a symmetric weight matrix. The gradient in (1) can be split into $-\frac{\partial E}{\partial x_{r\alpha}} = JV_r + F_{r\alpha} + Tx_{r\alpha}$, where $V_r = h_r - \sum_\beta x_{r\beta}$, $F_{r\alpha} = \sum_{r'} \mathsf{f}^\alpha_{rr'} x_{r'\alpha}$, and $-Tx_{r\alpha}$ are three basic interactions in the model, which can be interpreted with regard to the energy E:

JV_r: The *"vertical"* interaction JV_r implements a dynamical winner-take-all circuit within each col_r. Unlike in a standard penalty function, J should not be chosen large, but slightly above a critical value $J_c = \max_{r\alpha} \sum_{r'} \max(0, \mathsf{f}^\alpha_{rr'})$ which ensures convergence of the dynamics [Wersing et al., 1997] and allows for a modulation of the input h_r by the lateral interactions.

$F_{r\alpha}$: The lateral interaction $F_{r\alpha}$ couples activities within layers by the symmetric weight matrix $\mathsf{f}^\alpha_{rr'}$. The compatibility coefficients $\mathsf{f}^\alpha_{rr'} = \mathsf{f}(\nu_r, \nu_{r'})$ are a function of the feature parameters and determine which pattern configurations, if elicited as activity pattern within layers, will be mutually supporting among their constituent parts ($\mathsf{f}^\alpha_{rr'} > 0$) or instead suffer mutual inhibition ($\mathsf{f}^\alpha_{rr'} < 0$).

$Tx_{r\alpha}$: The self-inhibitory interaction $-Tx_{r\alpha}$ biases the minima of E towards ambiguous assignments. $T > 0$ can be regarded as a temperature, for very large T the global minimum of (2) is given by $x_{r\alpha} = h_r/L$, the maximally unassigned state. For $T \to 0$ the dynamics converges towards a proper consistent labeling. By gradually lowering T we can perform deterministic annealing to reduce probability of falling into local minima. T should be initialized to $T_c = \lambda_{max}\{f_{rr\prime}\}$ and then exponentially annealed to zero.

3 The application of the CLM to Contour Grouping in Fluorescence Micrographs of Cells

Contour grouping is an important objective for models of feature linking, where compatibilities between edge features generally express the degree of continuity of a curve passing over them. Synchronization-based

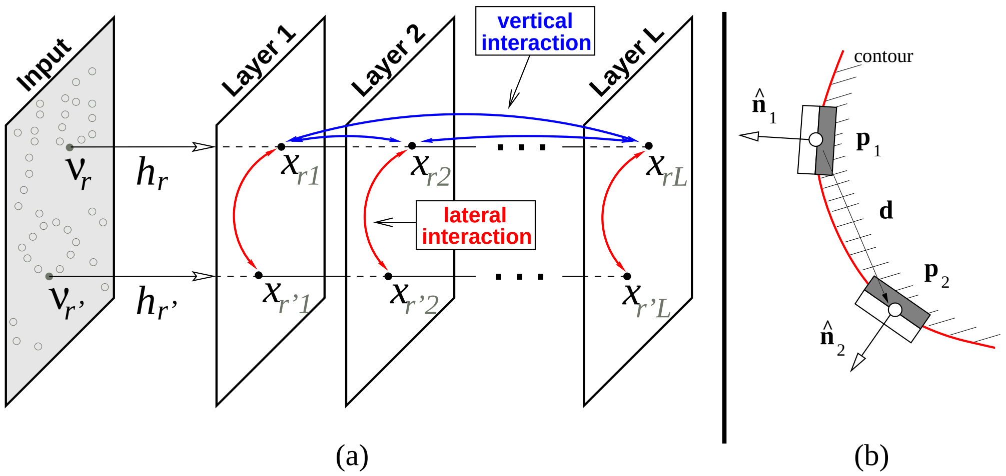

Figure 1: (a) The CLM architecture: Each neuron r of the input layer represents a particular image feature, in our case a local edge edge element parameterized by $\nu_r = (\mathbf{p}_r, \hat{\mathbf{n}}_r)$, where $\mathbf{p}_r$ is the position and $\hat{\mathbf{n}}_r$ is the orientation represented by a unit vector. In L replica layers of the input, each neuron represents the certainty of assigning feature r to this layer through its activity $\mathsf{f}^{\alpha}_{rr'}$ with α as the layer index. (b): The lateral interactions $\mathsf{f}^{\alpha}_{rr'}$ are computed from the edge parameters, and are dependent on the spatial difference vector $\mathbf{d}$ and the relative edge orientations calculated from $x, y-$gradients, illustrated by the white-grey boxes.

models, however, still face major difficulties in delivering a controllable grouping for the complex excitatory and inhibitory interactions as encountered in real world images. We will show now, how our approach can be used to combine a binding of salient contour groups with a mechanism of figure-ground segmentation.
In this application a feature r is described by the parameter vector $\nu_r = (\mathbf{p}_r, \hat{\mathbf{n}}_r)$ with $\mathbf{p}_r = (x_r, y_r)$ as its image position and $\hat{\mathbf{n}}_r$ as the unit orientation vector of its grey value gradient. The interaction function for binding features to cell contour groups is identically defined for all layers with exception of the first layer ($\alpha = 1$), referred to as the ground layer. Beside binding features to groups approximating cell contours, a figure-ground separation has to be performed. Therefore the ground layer is supplied with a separate interaction function to bind features of the background. The lateral interactions $\mathsf{f}^{\alpha}_{rr'}$ are given as follows: For the ground layer the lateral interactions are set to $\mathsf{f}^{1}_{rr'} = m\delta_{rr'}$. The parameter $m > 0$ defines a self-coupling against which lateral interactions in the figure layers must compete to make a feature "pop out" from the ground layer. In the rest of the layers ($\alpha > 1$) the lateral interaction $\mathsf{f}^{\alpha}_{rr'}$ of two features at positions $\mathbf{p}_1$ and $\mathbf{p}_2$ are computed from $\mathbf{d} = \mathbf{p}_1 - \mathbf{p}_2$ and their unit gradient orientation vectors $\hat{\mathbf{n}}_1 = (\hat{n}^x_1, \hat{n}^y_1)$, $\hat{\mathbf{n}}_2 = (\hat{n}^x_2, \hat{n}^y_2)$ (see Fig. 1(b)). The orientation (n^x_r, n^y_r) is computed by a standard x-sobel and y-sobel and normalized to unit length $(\hat{n}^x_r, \hat{n}^y_r) = \hat{\mathbf{n}}_r$. The lateral interaction $f(\nu_1, \nu_2)$ for two features is computed by

$$f(\nu_1,\nu_2) = \begin{cases} \theta(d)(\cos(\frac{d\pi}{2R} + \psi(\hat{\mathbf{n}}_1, \hat{\mathbf{n}}_2)^2) - I_g & \text{if } \hat{\mathbf{n}}_1 \hat{\mathbf{d}} < s \text{ and } \hat{\mathbf{n}}_2 \hat{\mathbf{d}} < -s \\ -\theta(d) I_l - I_g & \text{else} \end{cases}$$

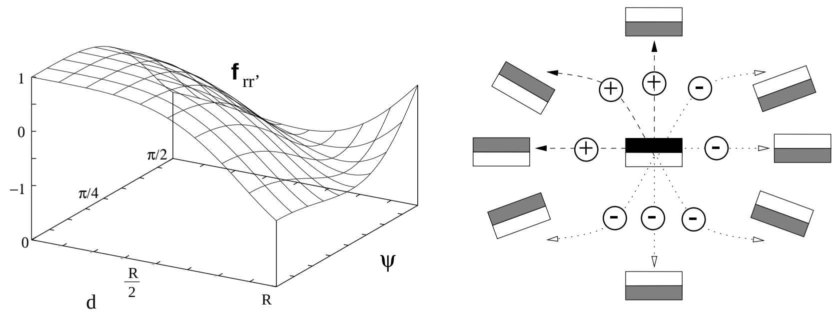

(a) interaction function

(b) lateral interaction between features

Figure 2: The lateral interaction function $f_{rr'}$: (a) The interaction function $f_{rr'}$ is plotted. Those feature pairs interact positively which are close located and have collinear and equally oriented gradient orientations or far distant and have collinear but reverse oriented gradients. (b) The lateral interactions of one edge feature (black/white-box) with a selection of others (grey/white-boxes) are illustrated. A positive interaction with one feature is illustrated by a plus-symbol, a negative one with a minus-symbol. One can see that convex continuation with a dark (inner) to light (outer) shading results in supporting interaction. Collinear gradients are only supported if they are reversely oriented.

with the euclidian feature distance $d = |\mathbf{d}|$ and the unit distance vector $\hat{\mathbf{d}} = \mathbf{d}/d$. $\theta(d)$ is 1 if the euclidean distance holds $d < R$, and 0 if not. The parameter R is a rough estimate of the cell diameter. The function $\psi(\hat{\mathbf{n}}_1, \hat{\mathbf{n}}_2) == \frac{\pi}{4}(1 - \hat{\mathbf{n}}_1 * \hat{\mathbf{n}}_2)$ measures the difference of the features' gradient orientations. The interaction supports gradient arrangements of two kinds. First, those pairs interact positively which are close enough and which have collinear and equally oriented gradients. Secondly, the more distant pairs of features interact positively, if their gradients are collinear but reverse oriented (see Fig. 2(b)), which supports the dynamics in grouping not only convex but *closed* structures together. The constant negative interaction value I_l is necessary to guarantee that two neighbored convex structures are not "merged" into one by grouping them both into one layer. The parameter s controls the sharpness of the convexity constraint. Parameters $I_g > 0$ and $I_l > 0$ control the strength of the global and local inhibition, respectively.

In the application to the fluorescence micrographs the input intensities h_r are set to 1 to make the grouping performance independent to variations of the gradients intensity along the cell contour. The constant J (see section 2) is set to J_c for contextual modulation, so contour elements of strong lateral support are enhanced and contour grouping performance is improved [Wersing and Ritter, 1999]. Annealing was started with setting the temperature to the maximum eigenvalue of the interaction matrix $T_c = \lambda_{max}\{\mathsf{f}_{rr'}\}$. Faster annealing leads to more fragmented groupings. Raising the ground layer coupling m from zero to higher values suppresses less salient groups, until at $m \approx J_c$ only the ground layer remains active. In this work the ground layer coupling is set to $m = 4.0$.

4 Results

The CLM contour grouping algorithm was applied to real images of size 64×64 and 128×128. The number of fluorescent lymphocyte cells in the images varied from 1 to 5 or 4 to 20 respectively. All images were processed with the same set of parameters. The CLM consisted of 20 layers plus one ground layer. The lateral interaction parameters were $s = 0.2, R = 9, I_l = 0.9, I_g = 0.5$. To compute a one-pixel wide cell contour from the group standard morphological operators are applied [Sonka et al., 1993]. The processing steps for three example images are shown in figure 3. As shown in figure 3 (d) it is readily seen that the cells contours are found including their ring of fluorescence. The grouping performance remains constant under local distortions in the convexity of the contour in grey value intensity.

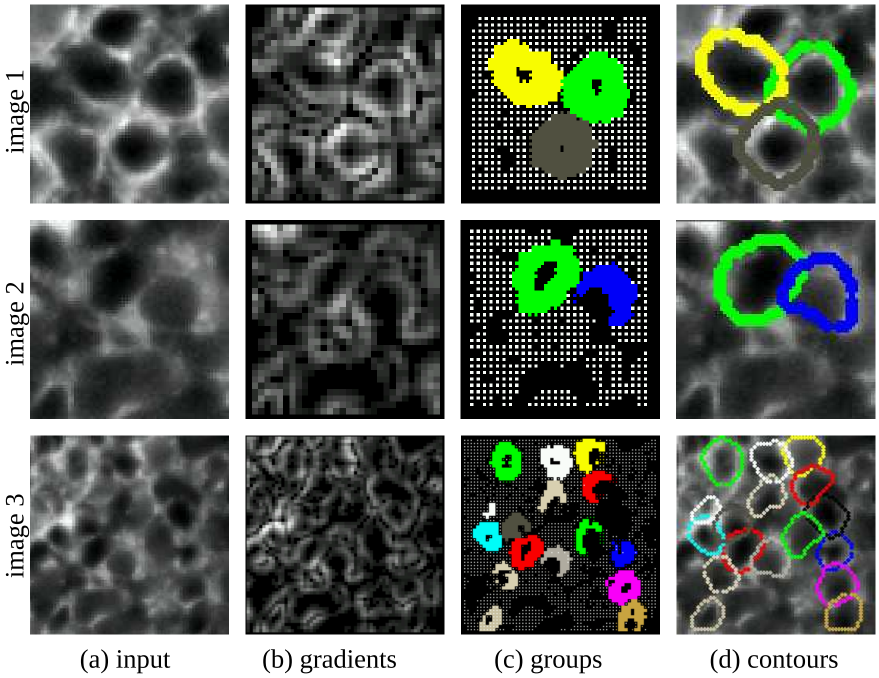

Figure 3: CLM contour grouping in fluorescence microscopy images: The input images (a) are subsampled by factor 2 and the the x,y-gradients are computed. Column (b) shows the superposition of the gradients' absolute values. In the third column the grouping results can be seen. The small white dots are the features which are assigned to the ground layer. Features with too small absolute valued gradients were omitted (black gaps). Grey boxes of same grey value are features which were grouped into the same layer. Although the CLM consisted of 20 layers the number of layers including a salient group is the same as the number of fluorescent cells, which would be selected by a biomedical expert. The column (d) shows the contours extracted from the grouping results. The bottom row shows that the algorithm can easily be applied on larger images (128×128). In this image the number of features is four times the number of features in image 1 and 2 and the annealing speed had to be lowered to get the presented result.

5 Conclusion

We showed how the concept of gestalt based feature binding with the CLM can be used for segmenting fluorescence micrographs of cells efficiently and with high accuracy. The approach unites figure-ground segmentation and grouping. The output consists of labeled image segments, each corresponding to a single salient cell. The grouping is robust due to the dynamical integration of noisy local curvature information into coherent salient groups. An important result of this study is that the number of groups need not be fixed in advance, and the setting can be applied to larger image patches without modification of the interaction parameters. The presented work was done in a close collaboration with the biomedical research group. The results were carefully inspected by the experts to measure accuracy and comparison with human performance. Discussions with the experts indicated that the CLM works with high accuracy and thereby provides one step forward to automatic evaluation of the microscope data.

Acknowledgments: This work was supported by DFG grant GK-231, SFB 387 (TPB1).

References

[Galbraith et al., 1991] Galbraith, W., Wagner, M., Chao, J., Abaza, M., Ernst, L., Nederlof, M., Hartsock, R., Taylor, D., and Waggoner, A. (1991). Imaging cytometry by multiparameter fluorescence. *Cytometry*, 12:579–596.

[Hanahara and Hiyane, 1990] Hanahara, K. and Hiyane, M. (1990). A circle-detection algorithm simulating wave propagation. *Machine Vision and Applications*, 3:97–111.

[Jacobs, 1996] Jacobs, D. W. (1996). Robust and efficient detection of salient convex groups. *IEEE Trans. on Pattern Analysis and Machine Intelligence*, 18(1):23–37.

[Kohler, 1959] Kohler, W. (1959). *Gestalt Psychology*. Mentor Books.

[Li, 1999] Li, Z. (August 1999). Contextual influences in v1 as a basis for pop out and asymmetry in visual search. *Proc. Nat. Acad. Sci. USA*, 96:10530–10535.

[Lowe, 1985] Lowe, D. (1985). *Perceptual Organization and Visual Recognition*. Kluwer Academic Puplishers.

[Meyer and Beucher, 1990] Meyer, F. and Beucher, S. (1990). Morphological segmentation. *J. Visual Communications and Image Representation*, 1(1):21–46.

[Ritter, 1990] Ritter, H. (1990). A spatial approach to feature linking. In *Int. Neur. Netw. Conf. Paris*.

[Sonka et al., 1993] Sonka, M., Hlavac, V., and Boyle, R. (1993). *Image Processing, Analysis and Machine Vision*. Chapman & Hall.

[Wersing and Ritter, 1999] Wersing, H. and Ritter, H. (1999). Feature binding and relaxation labeling with the competitive layer model. In *Proc. Eur. Symp. on Art. Neur. Netw. ESANN*, pages 295–300.

[Wersing et al., 1997] Wersing, H., Steil, J., and Ritter, H. (1997). A layered recurrent neural network for feature grouping. In Wulfram Gerstner, Alain Germond, M. H. and Nicoud, J.-D., editors, *Proc. Intern. Conf. on Art. Neur. Netw. Lausanne*, pages 439–444. Springer.

[Yen and Finkel, 1998] Yen, S.-C. and Finkel, L. H. (1998). Extraction of perceptually salient contours by striate cortical networks. *Vision Research*, 38(5):719–741.